



**FACULTY OF ELECTRICAL ENGINEERING
AND INFORMATION SCIENCE**



**INFORMATION TECHNOLOGY AND
ELECTRICAL ENGINEERING -
DEVICES AND SYSTEMS,
MATERIALS AND TECHNOLOGIES
FOR THE FUTURE**

Startseite / Index:

<http://www.db-thueringen.de/servlets/DocumentServlet?id=12391>

Impressum

Herausgeber: Der Rektor der Technischen Universität Ilmenau
Univ.-Prof. Dr. rer. nat. habil. Peter Scharff

Redaktion: Referat Marketing und Studentische
Angelegenheiten
Andrea Schneider

Fakultät für Elektrotechnik und Informationstechnik
Susanne Jakob
Dipl.-Ing. Helge Drumm

Redaktionsschluss: 07. Juli 2006

Technische Realisierung (CD-Rom-Ausgabe):
Institut für Medientechnik an der TU Ilmenau
Dipl.-Ing. Christian Weigel
Dipl.-Ing. Marco Albrecht
Dipl.-Ing. Helge Drumm

Technische Realisierung (Online-Ausgabe):
Universitätsbibliothek Ilmenau
[ilmedia](#)
Postfach 10 05 65
98684 Ilmenau

Verlag:  Verlag ISLE, Betriebsstätte des ISLE e.V.
Werner-von-Siemens-Str. 16
98693 Ilmenau

© Technische Universität Ilmenau (Thür.) 2006

Diese Publikationen und alle in ihr enthaltenen Beiträge und Abbildungen sind urheberrechtlich geschützt. Mit Ausnahme der gesetzlich zugelassenen Fälle ist eine Verwertung ohne Einwilligung der Redaktion strafbar.

ISBN (Druckausgabe): 3-938843-15-2
ISBN (CD-Rom-Ausgabe): 3-938843-16-0

Startseite / Index:
<http://www.db-thueringen.de/servlets/DocumentServlet?id=12391>

M. Bjekic

Numerical Simulation, Measuring and Foreseeing Dynamic Characteristics of the Energetic Permanent Magnet Step Motor

INTRODUCTION

This paper analyzes dynamic characteristics of the eight-pole three-phase permanent magnet step motor.

The requirements for the construction of such a motor are that:

- a) the construction is cheap, and
- b) it develops electromagnetic torque needed to open and close the valves for liquid and gas (Fig. 1).

This is the reason why the stator is taken from classic three-phase asynchronous motor (Fig. 2) and the rotor is designed so that permanent ceramic magnets are attached to non-magnetic core (Fig. 3.) or ferromagnetic core (Fig. 4).

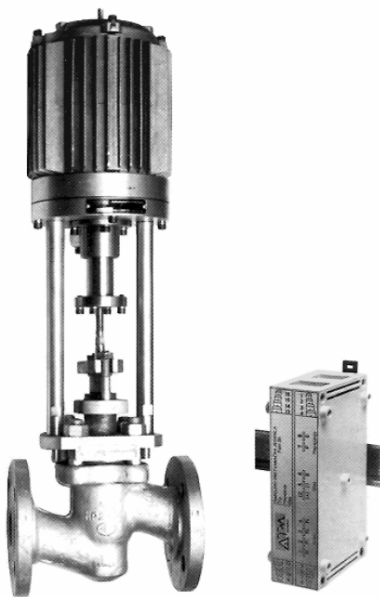


Fig. 1 – *Permanent magnet step motor drive*

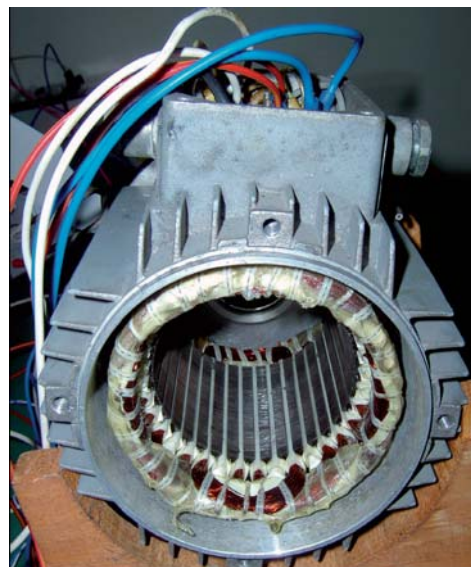


Fig. 2 – *Step motor stator*

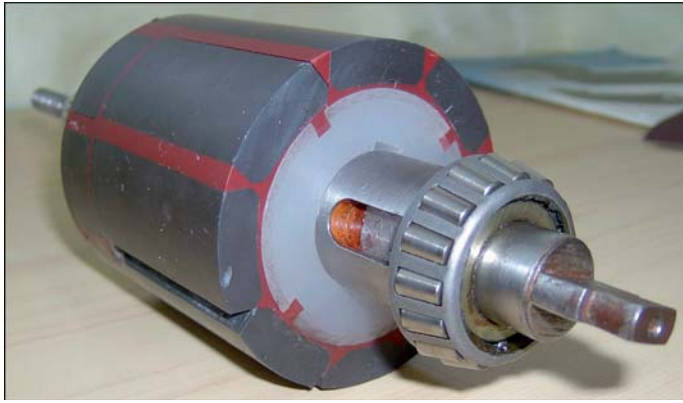


Fig. 3 – *Non-magnetic rotor*



Fig. 4 – *Ferromagnetic rotor*

SOLVING STEP MOTOR MAGNETIC CIRCUIT USING FINITE ELEMENT METHOD

The programme package FEMM is used to solve magnetic circuit of step motor [1]. Figure 5 shows magnetic circuit cross-section, divided by mesh including 22.871 nodes and 45.651 elements.

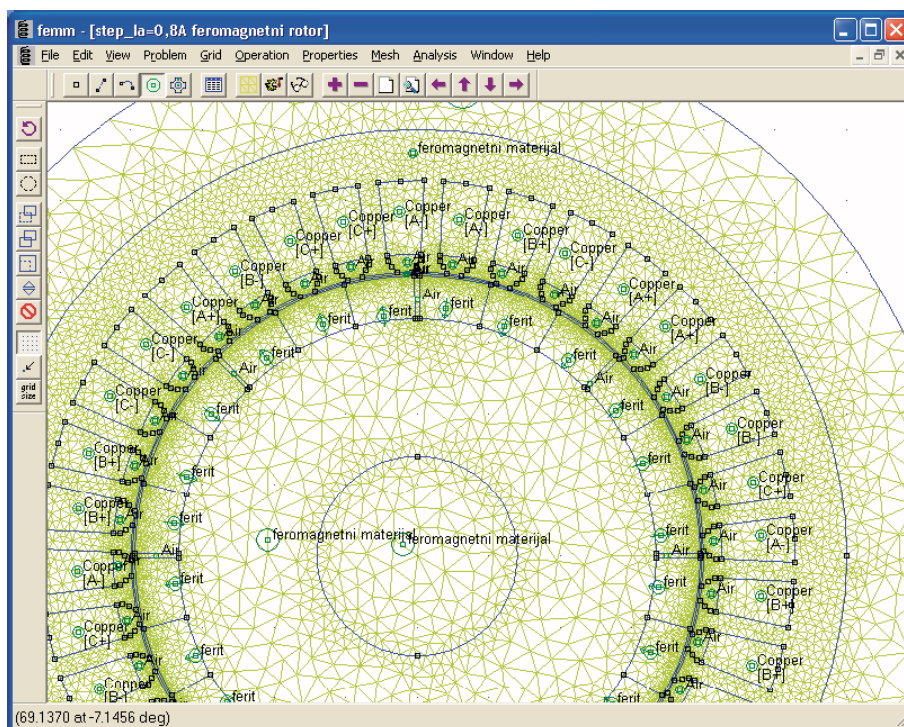


Fig. 5 - *Magnetic circuit divided by triangular mesh*

Figure 6 illustrates solving FEM simulation: magnetic flux density and magnetic field lines of part of magnetic circuit.

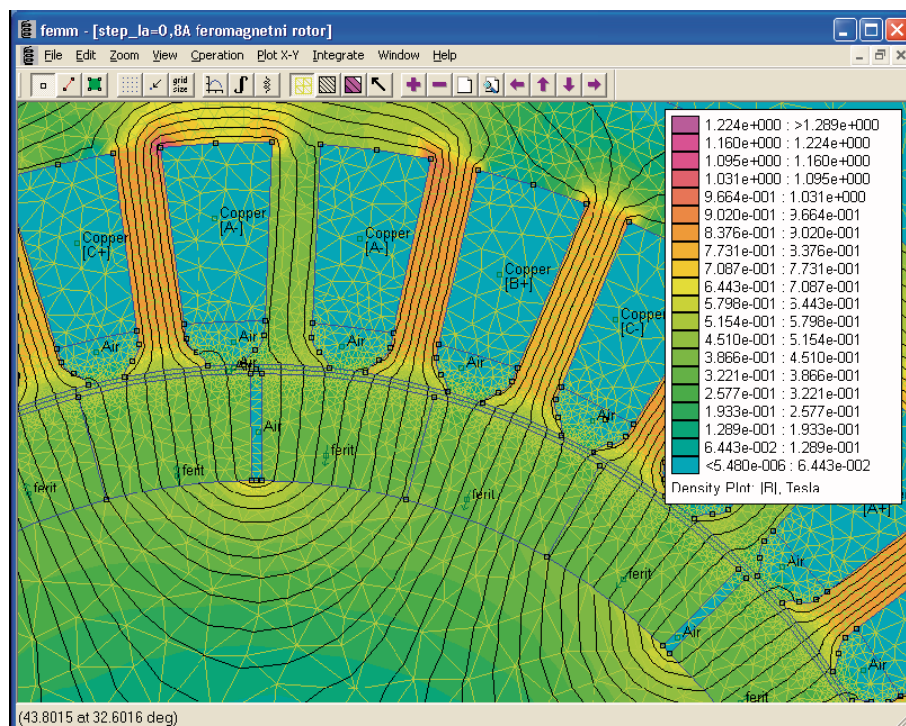


Fig. 6 - Magnetic flux density and magnetic field lines of part of magnetic circuit

By using this method we obtained the following data necessary for dynamic simulation:

- Static torque of the motor for all the rotor positions (Fig. 7).

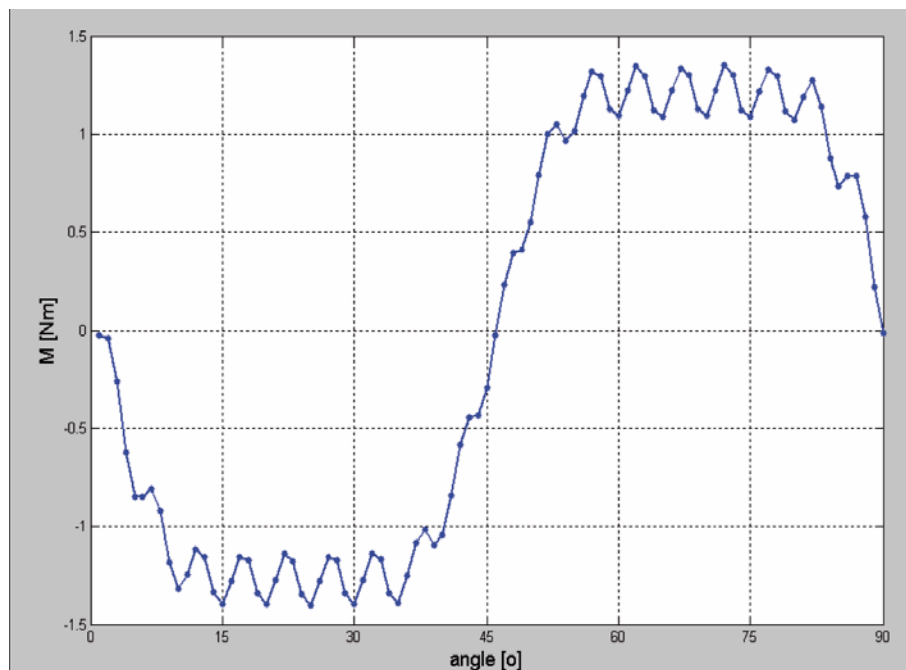


Fig. 7 - $M_1=f(\theta)$ FE rotor $I_1=0,8A$ $I_2=0A$ $I_3=0A$

- Self-inductance (Fig. 8) and mutual inductance (Fig. 9) of the coils. The simulation determined at which boundary stator current values the magnetic field can be considered as linear, which enables the simplified simulation procedure.

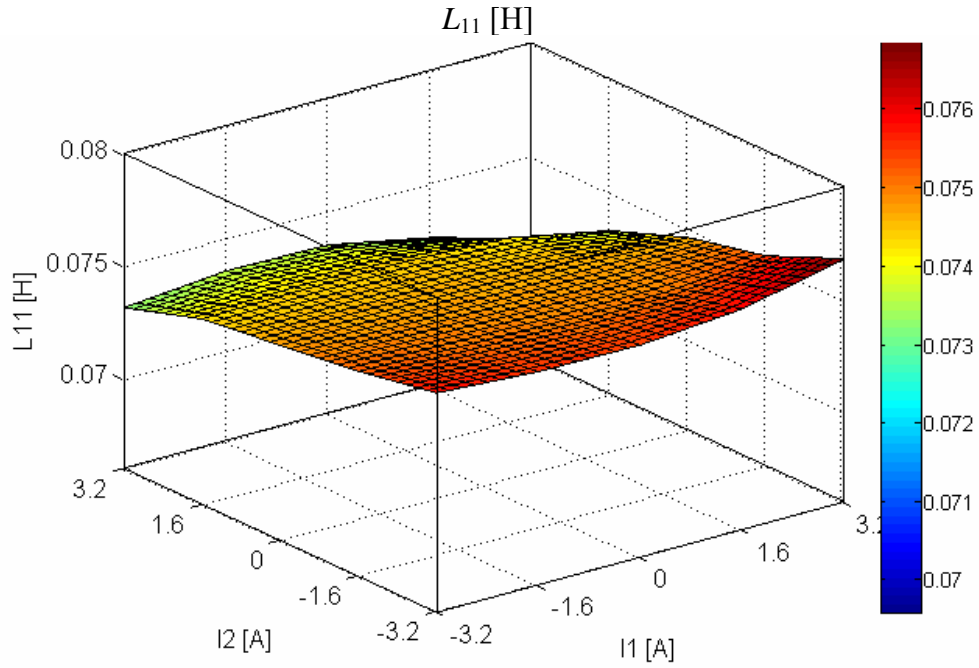


Fig. 8 - $L_{11}=f(I_1, I_2)$ $\theta = 0$ [°], FE rotor

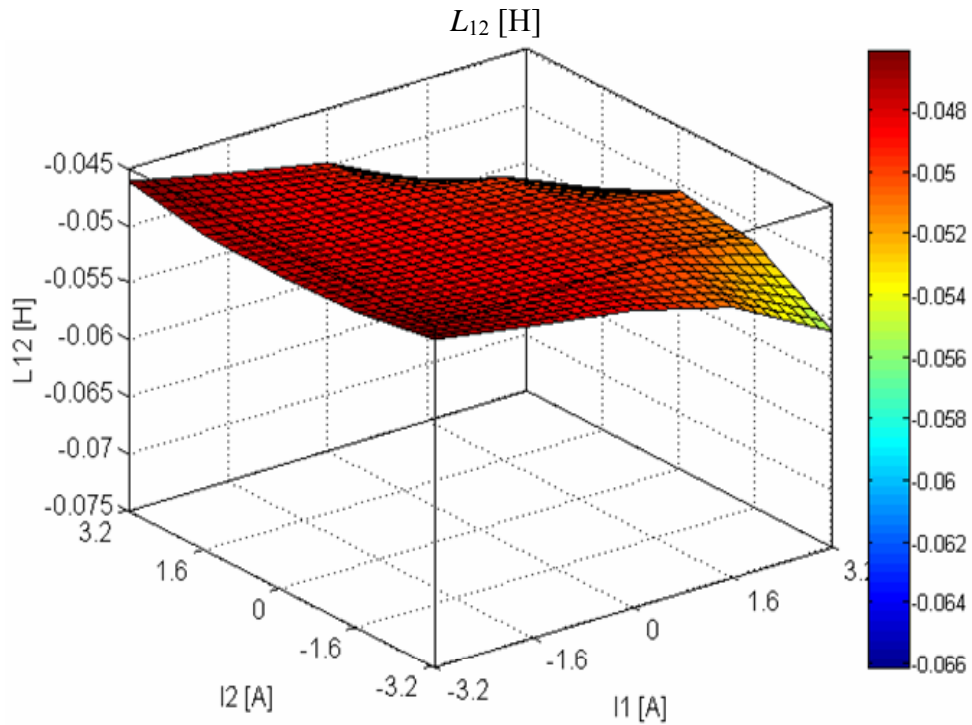


Fig. 9 - $L_{12}=f(I_1, I_2)$, $\theta = 0$ [°], FE rotor

Figure 10 shows 3D graph illustrating dependence of electromagnetic torque on all three stator currents for balance rotor position when exciting stator first phase (rotor angle is $\theta = 0$ [°]).

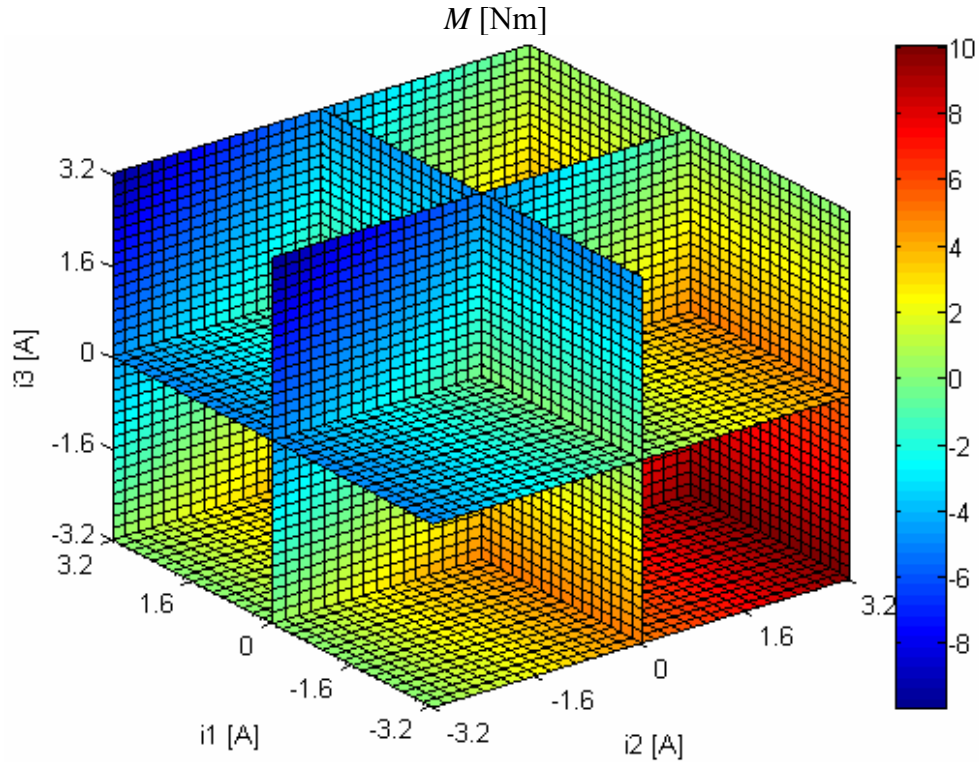


Fig. 10 - $M=f(I_1, I_2, I_3)$ $\theta = 0^\circ$ $3,2 \text{ A} < (i_1, i_2, i_3) < 3,2 \text{ A}$ FE rotor

ANALYTICAL EQUATION OF DEVELOPED STATIC TORQUE

Trigonometric collocation polynomial is used for obtaining analytical equation of developed static torque. The paper shows the equation (1-7) that is used in dynamic simulation [1].

$$M(\theta) = \sum_{i=1}^3 C_i(\theta) i_i + M_{\text{rel}}(\theta) \quad (1)$$

$$C_i(\theta) = 130 \frac{180}{\pi} (\psi_{fi}(\theta'') - \psi_{fi}(\theta')) \quad (2)$$

$$M_{\text{rel}}(\theta) = B_{18} \sin(18\theta) \quad (3)$$

$$C_i(\theta) = B_{i1} \sin(\theta) + B_{i3} \sin(3\theta) + B_{i5} \sin(5\theta) + B_{i15} \sin(15\theta) + B_{i17} \sin(17\theta) + A_{i1} \cos(\theta) + A_{i3} \cos(3\theta) + A_{i5} \cos(5\theta) + A_{i15} \cos(15\theta) + A_{i17} \cos(17\theta) \quad (4)$$

$$\mathbf{i} = \mathbf{A}^{-1} \mathbf{B} \quad (5)$$

$$A = \begin{bmatrix} R_1 + \frac{L_{11}}{\Delta t} & \frac{L_{12}}{\Delta t} & \frac{L_{13}}{\Delta t} \\ \frac{L_{21}}{\Delta t} & R_2 + \frac{L_{22}}{\Delta t} & \frac{L_{23}}{\Delta t} \\ R_3 + \frac{L_{33}}{\Delta t} & \frac{L_{31}}{\Delta t} & \frac{L_{32}}{\Delta t} \end{bmatrix} \quad (6)$$

$$B = \begin{bmatrix} U_1 + \frac{L_{11}}{\Delta t} i_{10} + \frac{L_{12}}{\Delta t} i_{20} + \frac{L_{13}}{\Delta t} i_{30} - \frac{\psi_{f1} - \psi_{f10}}{\Delta t} \\ U_2 + \frac{L_{21}}{\Delta t} i_{10} + \frac{L_{22}}{\Delta t} i_{20} + \frac{L_{23}}{\Delta t} i_{30} - \frac{\psi_{f2} - \psi_{f20}}{\Delta t} \\ U_3 + \frac{L_{31}}{\Delta t} i_{10} + \frac{L_{32}}{\Delta t} i_{20} + \frac{L_{33}}{\Delta t} i_{30} - \frac{\psi_{f3} - \psi_{f30}}{\Delta t} \end{bmatrix} \quad (7)$$

Table 1 shows the calculated coefficients A_v and B_v by means of which electromagnetic torques for each phase are calculated. Table 2 shows the coefficient for calculating reluctance torque.

Tab. 1 - Calculated coefficients A_v and B_v

			v=1	v=3	v=5	v=15	v=17
M_{f1}	PVC rotor	A_v	-0.00012	-0.00017	-0.00035	0.00018	0.00011
		B_v	-1.38098	-0.34276	-0.05325	0.01515	0.02060
M_{f1}	FE rotor	A_v	-0.00023	-0.00021	-0.00019	0.00012	0.00006
		B_v	-1.83730	-0.35576	-0.05346	0.01558	0.02316
M_{f2}	PVC rotor	A_v	1.19604	-0.00020	-0.00461	0.00004	0.01753
		B_v	0.69018	-0.34260	0.00265	0.01547	-0.01070
M_{f2}	FE rotor	A_v	1.59145	-0.00021	-0.04626	0.00002	0.01998
		B_v	0.91831	-0.35578	0.02663	0.01550	-0.01185
M_{f3}	PVC rotor	A_v	-1.19565	-0.00027	0.04622	0.00025	-0.01793
		B_v	0.69060	-0.34251	0.02646	0.01597	-0.01040
M_{f3}	FE rotor	A_v	-1.59086	-0.00021	0.04621	0.00002	-0.02013
		B_v	0.91887	-0.35558	0.02656	0.01550	-0.01156

Tab. 2 - Coefficient for calculating reluctance torque

			v=18
M_{rel}	PVC rotor	B_{18}	-0.12811
M_{rel}	FE rotor	B_{18}	-0.13614

Figure 11 illustrates the calculated torque values of each phase for both rotor types, at the stator exciting currents $I_1=0,8$ A, $I_2=0$ A and $I_3=0$ A.

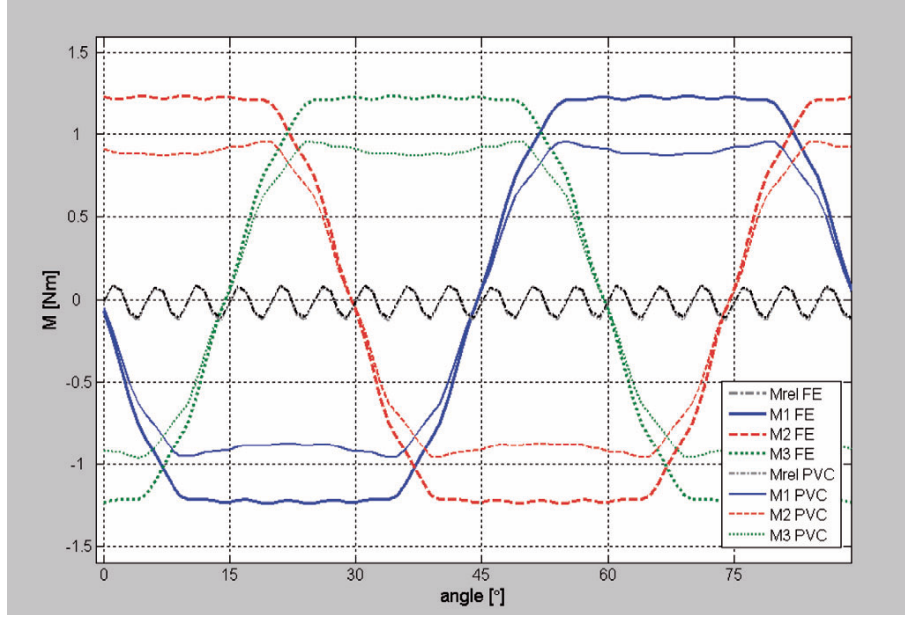


Fig. 11 – Calculated torque values of each phase for both rotor types for $I_l=0,8$ A

SOLVING DYNAMIC EQUATION OF MOTION WITH VARIABLE COEFFICIENTS

The concept of new numerical simulation is as follows: for each moment in time, differential equation of the second degree (8) is evaluated but with variable coefficients (with initial conditions relevant only for that single moment in time).

$$J \frac{d^2\theta}{dt^2} + F \frac{d\theta}{dt} = M(t, \theta) - M_{\text{load}} \quad (8)$$

The programme of transient state simulation consists of 3 units:

1- Data entry:

- motor data:** windings resistance ($R = 30 \Omega$), self and mutual inductances ($L_{fe}=0,074706$ H $M_{fe}=-0,049165$ H), moment of inertia J and friction coefficient F ($J_{fe}=0,00086$ kg m^2 , $F_{fe}=0,05$ Nm²/(rad/s), and reduced load torque $J_{\text{load}}=0,01$ Nm²/(rad/s), coefficients A_i and B_i ($i=1, 3, 5, 15$ and 17) for calculating coefficients $C_1, C_2, C_3, M_{\text{rel}}, \psi_{f1}, \psi_{f2}$ and ψ_{f3} .
- working regime data:** plug-in voltage ($U=18$ V), impulse duration ($\Delta T=5$ s), load torque and its character (active or reactive) ($M_{\text{load}}=0,5$ Nm), initial angle and initial rotation speed ($\theta_0=0$ rad $\omega_0=0$ rad/s), sequence of exciting the phases, number of positions per step ($N=500, \Delta t=\Delta T/500 = 6$ ms).

- 2- **Work – solving the equations.** This part of the programme was to solve dynamic movement equation in which its coefficients were changed for each new position.
- 3- **The results.** Figures 16 and 17 illustrate the obtained simulation results.

APPARATUS SET FOR MEASUREMENT

In order to confirm the obtained simulated results, several measurements were carried out.

Apparatus set for measurement is shown in Fig. 12. To one side of the rotor of step motor (1) a disc is attached (2). The disc loads the motor with the active torque by using weights (3). An immobile optical mouse (4), which registers the rotor motion, leans on the disc. Through the acquisition card the computer gives digital signals to the control unit (5) which excites the stator windings of step motor according to the predetermined sequence. The acquisition system (6) is used simultaneously to record voltages and currents in all the three phases of the step motor. The monitor screen (7) shows instantaneously measured values.

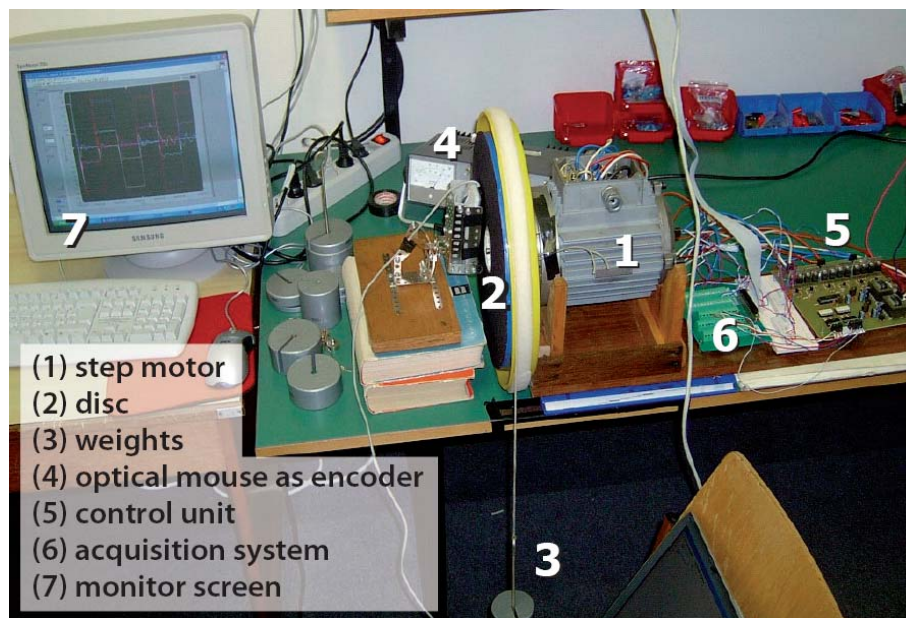


Fig. 12 -Apparatus set for measurement

Figure 13 illustrates the connection of the OMRON absolute encoder E6C3-AG5C with 1024 resolution (1) and three-phase eight-pole step motor. The motor is fed through the rectifier (2) and control unit (3) which received generated digital

signals via acquisition card NI 6013 (4). The motor is excited by the simultaneous switching on of one or two phases of the three-phase stator in the precisely defined sequence and current direction.

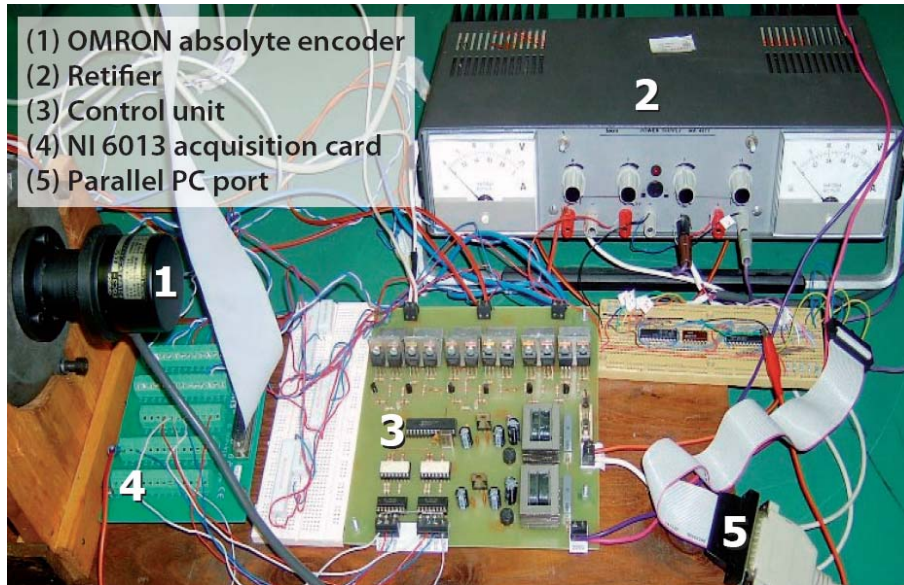


Fig. 13 - Drive circuit and acquisition system

In order to receive ten-bit digital signal from absolute optical encoder, 379 status register of parallel port (5) is used. The problem is that parallel port contains only 5 input bits of status register. Electronic circuit (Fig. 14) was created to receive five-bit signal and process them through the acquisition card in LABVIEW program, so that the parallel port could receive ten-bit signal.

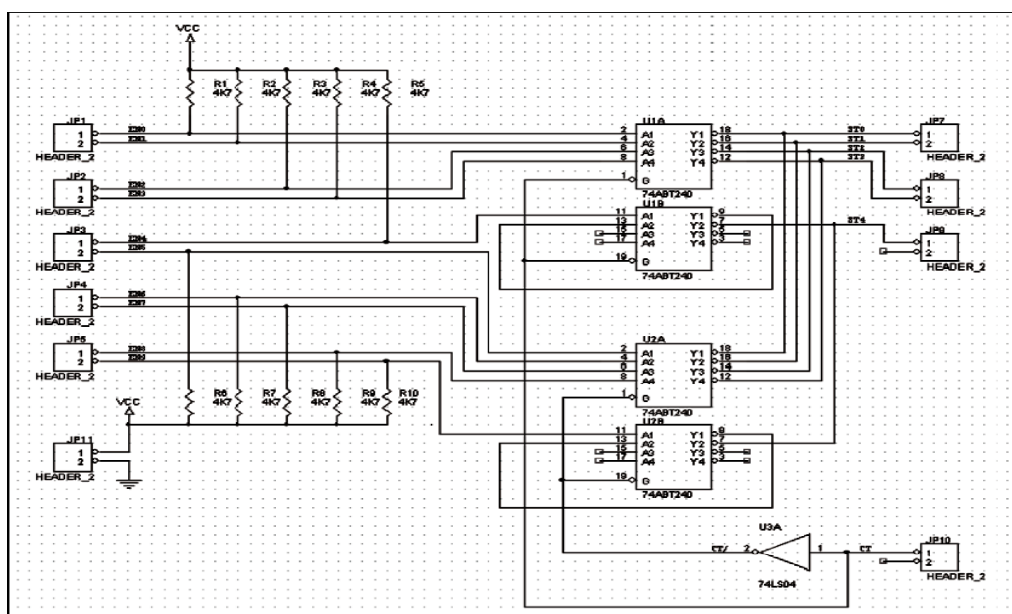


Fig. 14 - Scheme of electronic circuit for receiving 10-bit signal of optical encoder by means of 5-bit status register of parallel port

Figure 15 shows the front panel of LABVIEW programme which measures values voltages, current and rotor position.

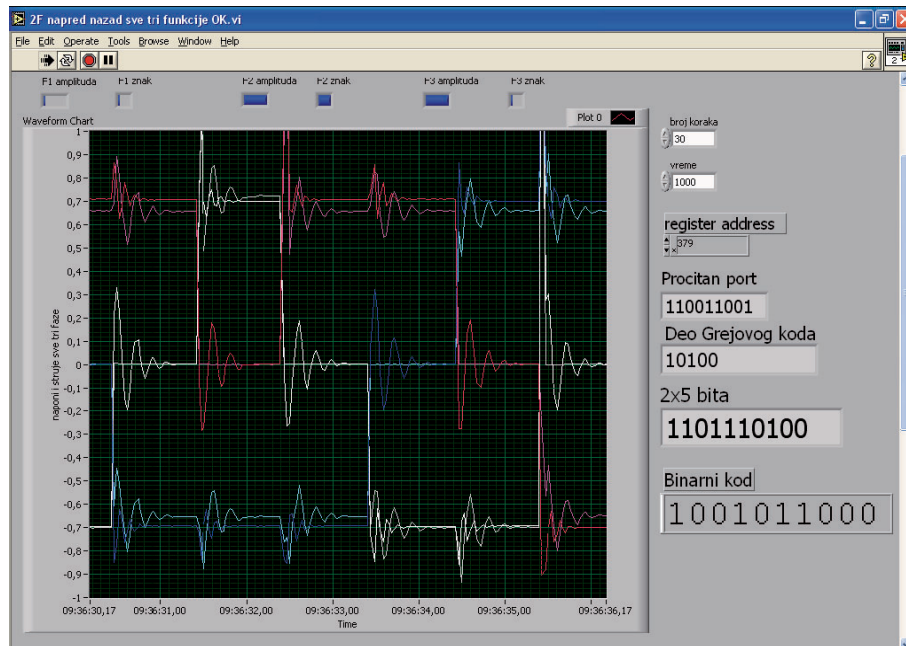


Fig. 15 - Measure values voltages, current and rotor position

SIMULATED AND MEASURED VALUES OF MOTION DYNAMIC CHARACTERISTICS

Simulated and measured values were compared, which confirmed the accuracy of the simulation procedure. Figures 16 and 17 illustrate the simulated values of voltages, currents, the positions of rotor and developed torques of each phase.

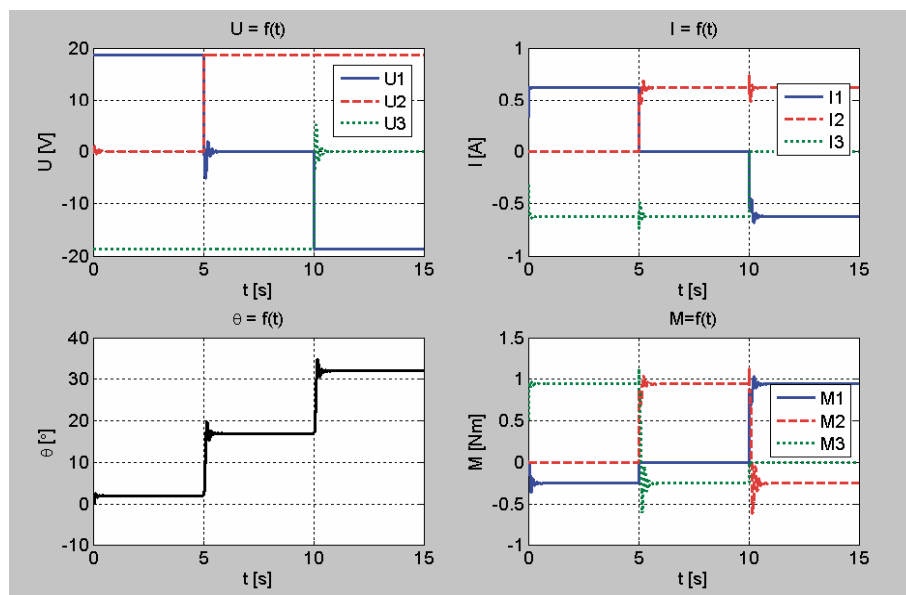


Fig. 16 - Simulated values of voltages, currents, the positions of rotor and torques of each phase

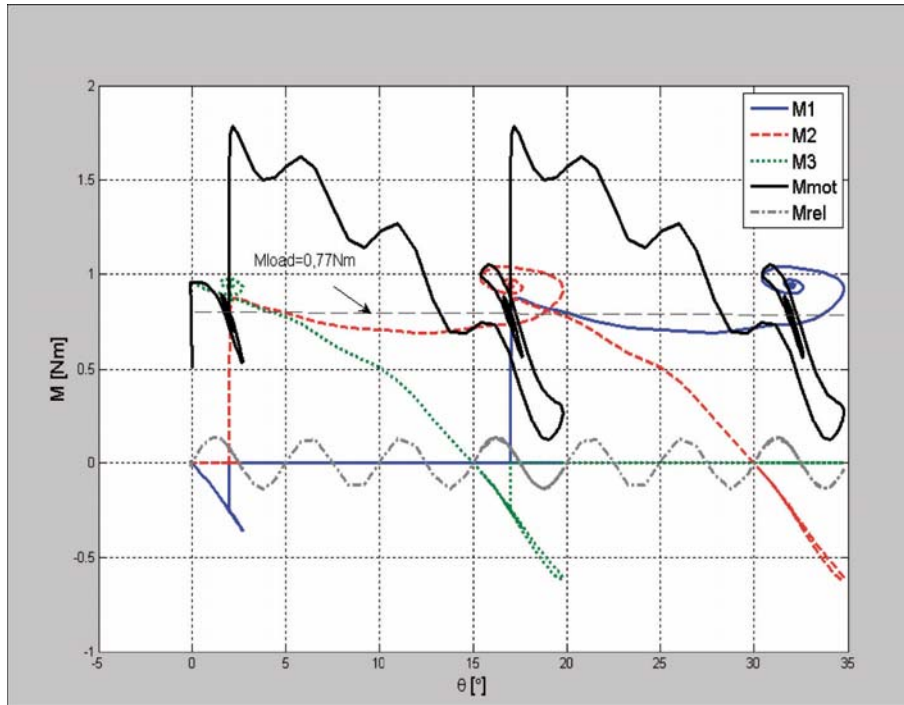


Fig. 17 - M_{mot} , M_{rel} , M_1 , M_2 , $M_3 = f(\theta)$

Figure 18 shows the simulated and measured values of rotor positions during its step movement.

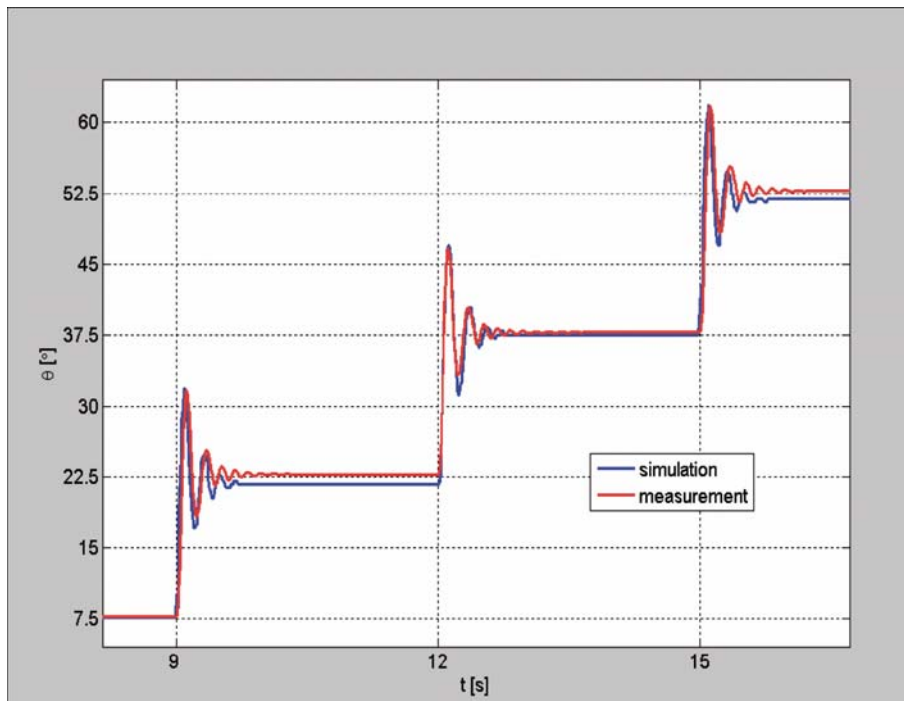


Fig. 18 - $\theta = f(t)$ (FE rotor, 2 phase excited, $M_{load} = 0$ Nm, $\Delta t = 3$ s)

We obtained pull-out characteristics as the most significant result of the simulation. This characteristics was also measured. Figure 19 gives parallel illustration of these values.

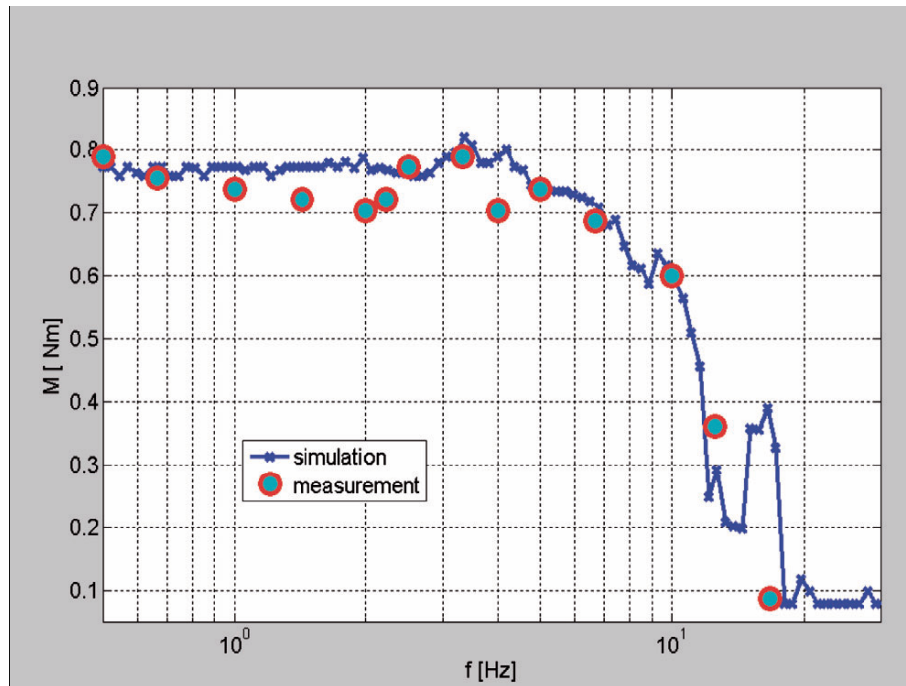


Fig. 19 - *Non-magnetic rotor, 2 phases simultaneously excited
 $I_n = 0,8 \text{ A}$, pull-out characteristic*

SUGGESTION FOR NEW ENERGETIC PERMANENT MAGNET STEP MOTOR AND ITS TORQUE CHARACTERISTICS

The simulation and measurement having been carried out, the construction was optimized and new energetic permanent magnet step motor was suggested. The new construction provides pull-out characteristics higher than the pull-out characteristics of previously constructed motor, which is the fundamental requirement for its construction optimization.

The modifications of construction include the following: the length of permanent magnets is increased; the construction with ferromagnetic ring instead of ferromagnetic core (whose moment of inertia was relatively high) was suggested. In this way the value of magnetic inductance in air gap of magnetic circuit remained the same, while the value of rotor moment of inertia was considerably decreased. Besides, the increase of exciting stator currents at new nominal value was also suggested after the necessary thermic measurements were carried out in order to determine new nominal values of the stator currents.

Figure 20 shows the solved magnetic circuit. This figure also shows that the magnetic circuit maintained linear working regime.

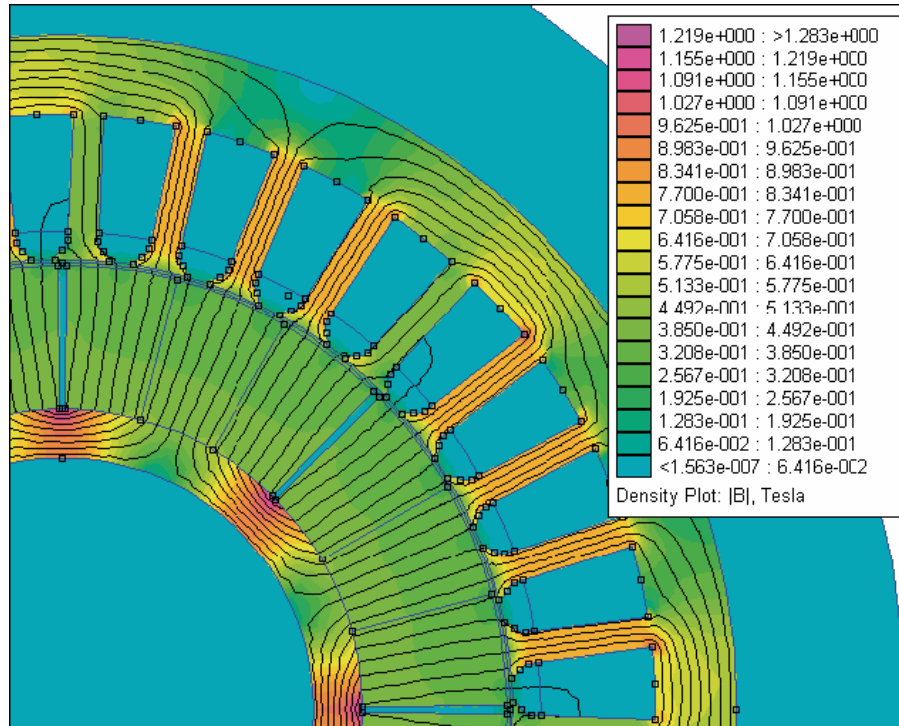


Fig 20. – Solved magnetic circuit of new step motor

Finally, Pull-in and Pull-out characteristics of the old and new step motor were compared (Fig. 21). The new step motor can operate at higher frequencies and can be loaded by higher load torque.

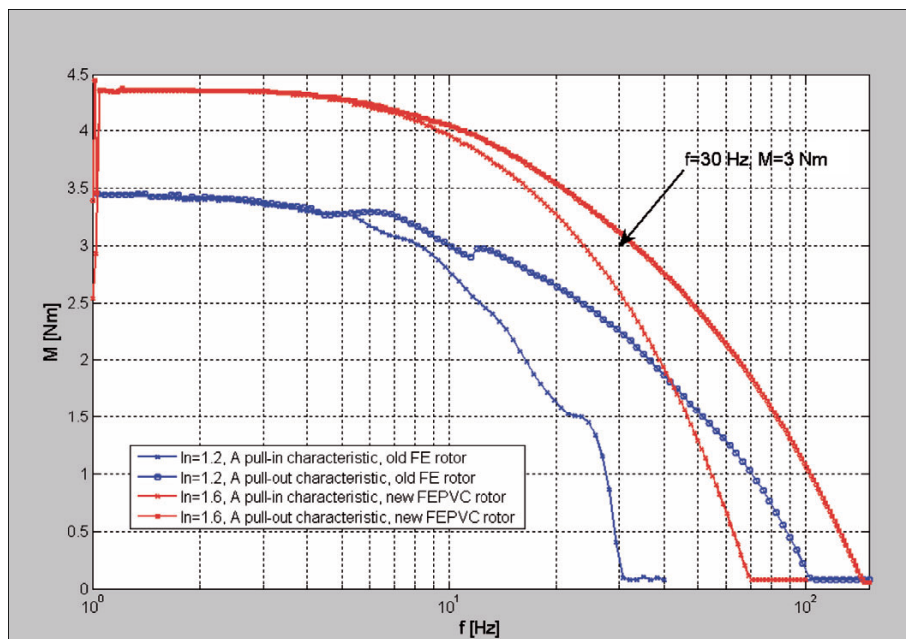


Fig. 21 - Pull-in and Pull-out characteristics: old FE rotor and new FE PVC rotor

The simulated results of the developed torque for each stator phase at step movement frequency $f = 30$ Hz and load torque $M_{\text{load}} = 3$ Nm were shown as the example of the simulation (Fig. 22).

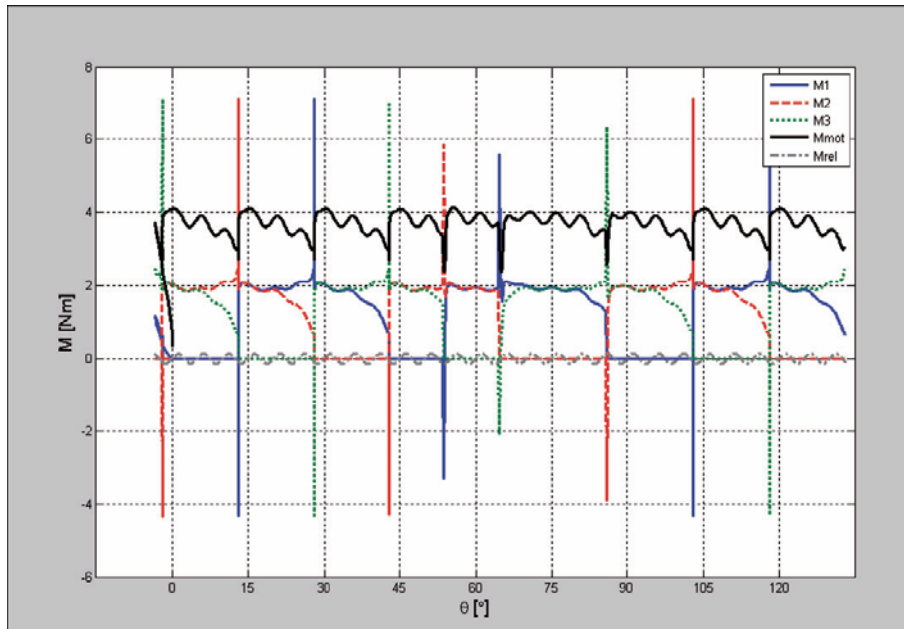


Fig. 22 - $M_{\text{mot}} = f(\theta)$ $f = 30$ Hz, $M_{\text{load}} = 3$ Nm

CONCLUSION

This paper analyzes numerical simulation, measuring and foreseeing dynamic characteristics of the energetic permanent magnet step motor. Considering the actual step motor, simulations and measurements confirmed the accuracy of the simulation procedure. By using newly developed procedure, we suggested the completely new construction of step motor with better working characteristics.

References:

- [1] M. Bjekic: "Numerical method of solving magnetic circuit of permanent magnet step motor", Computation of Electromagnetic Field, International PhD seminar, 2004, Budva, pp. 11-16
- [2] M. Bjekic: "Numerical computation dynamic characteristics of permanent-magnet step motor", Numerical Field Computation and Optimization in Electrical Engineering, International PhD seminar, 2005, Ohrid, pp. 11-16

Authors:

Miroslav M. Bjekic
 Technical faculty of Cacak, Svetog Save 65
 32000, Cacak, Serbia
 Phone: +381 32 302 762
 Fax: +381 32 342 101
 E-mail: mbjekic@ptt.yu